Application of an *hp*-adaptive FE method for computing electromagnetic scattering in the frequency domain

N. Sehlstedt*, A. Zdunek§ and W. Rachowicz‡

*Swedish Defence Research Agency, SE-172 90 Stockholm, Sweden, stn@foi.se
§Swedish Defence Research Agency, SE-172 90 Stockholm, Sweden, zka@foi.se
‡PK, Cracow University of Technology, Cracow, Poland, waldek@mlody.zms.pk.edu.pl

Abstract

Herein the electromagnetic scattering is determined using the Finite Element Method. In particular the radar cross section of the scatterer is estimated. Comparison between the Finite Element Method (FEM), Method of Moments (MoM) and the method of Physical Optics (PO) is made in one numerical example. In another numerical example, the convergence rate is compared using pure h-refinement, p-enrichment and with a priori hp-adaptive refinements. The gain using the hp-adaptive approach is significant since an exponential convergence may be obtained.

1 Introduction

Accurate calculations of the electromagnetic scattering from objects is of great importance in the design of low observable, so-called, stealth vehicles. External scattering from electrically large convex objects is usually estimated by means of high frequency methods, such as the method of physical optics. So called numerically exact methods, such as method of moments, finite difference and/or the finite element method are preferable whenever it is possible.

Here the electromagnetic scattering, expressed in terms of radar cross section (RCS), is calculated using an hp-adaptive finite element method. The hp-adaptive method, where the elements have locally variable order of approximation p and element size h, is very suitable for modeling singularities such as those resulting from irregular geometries. Also, the numerical dispersion error, e.g. in resonating cavities, may be reduced using the hp-method. The ability to model singularities, is one of the largest advantages for using the hp-method, since the maximal convergence may be retained. The hp-adaptive FE code used here, called EM3D, is a derivative of a general package for hp-adaptive FE discretizations called 3Dhp90, see [1]. EM3D has extensively been applied in cavity problems, see e.g. [2]; herein focus will be made solely on the scattering from a compact body in the free space.

2 Problem statement

Consider the following formulation of the time-harmonic Maxwell's equations in terms of the *scattered* electric field $\boldsymbol{E}$ defined as $\boldsymbol{E} := \boldsymbol{E}^{tot} - \boldsymbol{E}^{inc}$, where $\boldsymbol{E}^{tot}$ is the total electric field and $\boldsymbol{E}^{inc}$ is the incident electric field. Let Ω be a open, bounded domain $\Omega \subset \mathbb{R}^3$, with boundary Γ surrounded by the free space $\Omega^+ := \mathbb{R}^3 \backslash \bar{\Omega}$. Let also the exterior domain Ω^+ be truncated by introducing an artificial, closed boundary Γ_0, and denote the part of the reduced exterior by Ω_0^+ and the enclosed remaining part of Ω^+ by Ω_0, i.e. $\Omega^+ := \Omega_0 \cup \Omega_0^+$. Then the problem is to find the scattered electric field $\boldsymbol{E}(\boldsymbol{x})$, $\boldsymbol{x} \in \bar{\Omega} \cup \Omega_0$, such that

$$\boldsymbol{\nabla} \times \left(\frac{1}{\mu_r} \boldsymbol{\nabla} \times \boldsymbol{E} \right) - k_0^2 \hat{\epsilon}_r \boldsymbol{E} = -jk_0 Z_0 \boldsymbol{J}^{imp} \tag{1}$$

is satisfied. In the above $\hat{\epsilon}_r := \epsilon_r(1 - j\frac{\sigma}{\omega\epsilon})$ and μ_r, ϵ_r and σ are relative permittivity, relative permeability and conductivity respectively; and ω is the circular frequency. Also, in the above equation $k_0 := \omega\sqrt{\epsilon_0\mu_0}$

Report Documentation Page

Form Approved
OMB No. 0704-0188

Public reporting burden for the collection of information is estimated to average 1 hour per response, including the time for reviewing instructions, searching existing data sources, gathering and maintaining the data needed, and completing and reviewing the collection of information. Send comments regarding this burden estimate or any other aspect of this collection of information, including suggestions for reducing this burden, to Washington Headquarters Services, Directorate for Information Operations and Reports, 1215 Jefferson Davis Highway, Suite 1204, Arlington VA 22202-4302. Respondents should be aware that notwithstanding any other provision of law, no person shall be subject to a penalty for failing to comply with a collection of information if it does not display a currently valid OMB control number.

1. REPORT DATE **01 JAN 2005**	2. REPORT TYPE **N/A**	3. DATES COVERED -

4. TITLE AND SUBTITLE **Application of an hp-adaptive FE method for computing electromagnetic scattering in the frequency domain**	5a. CONTRACT NUMBER 5b. GRANT NUMBER 5c. PROGRAM ELEMENT NUMBER
6. AUTHOR(S)	5d. PROJECT NUMBER 5e. TASK NUMBER 5f. WORK UNIT NUMBER
7. PERFORMING ORGANIZATION NAME(S) AND ADDRESS(ES) **Swedish Defence Research Agency, SE-172 90 Stockholm, Sweden**	8. PERFORMING ORGANIZATION REPORT NUMBER
9. SPONSORING/MONITORING AGENCY NAME(S) AND ADDRESS(ES)	10. SPONSOR/MONITOR'S ACRONYM(S) 11. SPONSOR/MONITOR'S REPORT NUMBER(S)

12. DISTRIBUTION/AVAILABILITY STATEMENT
Approved for public release, distribution unlimited

13. SUPPLEMENTARY NOTES
See also ADM001846, Applied Computational Electromagnetics Society 2005 Journal, Newsletter, and Conference., The original document contains color images.

14. ABSTRACT

15. SUBJECT TERMS

16. SECURITY CLASSIFICATION OF:			17. LIMITATION OF ABSTRACT	18. NUMBER OF PAGES	19a. NAME OF RESPONSIBLE PERSON
a. REPORT **unclassified**	b. ABSTRACT **unclassified**	c. THIS PAGE **unclassified**	**UU**	**4**	

is the wavenumber in free space, and $Z_0 = \sqrt{\mu_0/\epsilon_0}$ is the intrinsic impedance of free space. In Eq. (1) $\boldsymbol{J}^{imp}$ is the impressed current defined as

$$\boldsymbol{J}^{imp} := \left(\hat{\epsilon}_r - \frac{1}{\mu_r}\right) j\omega\epsilon_0 \boldsymbol{E}^{inc}, \qquad \boldsymbol{E}^{inc}(\boldsymbol{x}) := E_0\, \boldsymbol{p}\, e^{-j\, k_0\, \boldsymbol{d}\cdot\boldsymbol{x}}. \tag{2}$$

In the above E_0 is the amplitude, $\boldsymbol{p}$ is a unit vector identifying the polarization of the incident field, and $\boldsymbol{d}$ is the direction of propagation.

At a perfect electrical conductor (PEC) surface Γ the non-homogeneous Dirichlet boundary condition

$$\boldsymbol{n} \times \boldsymbol{E} = -\boldsymbol{n} \times \boldsymbol{E}^{inc}, \tag{3}$$

is imposed; $\boldsymbol{n} = \boldsymbol{n}(\boldsymbol{x})$ is the unit vector normal to Γ at a point $\boldsymbol{x}$. At material interfaces the following continuity conditions are applied

$$\boldsymbol{n} \times [\![\boldsymbol{E}]\!] = -\boldsymbol{n} \times \left[\!\left[\boldsymbol{E}^{inc}\right]\!\right], \qquad \boldsymbol{n} \times \left[\!\left[\frac{1}{\mu_r}\nabla \times \boldsymbol{E}\right]\!\right] = -\boldsymbol{n} \times \left[\!\left[\frac{1}{\mu_r}\right]\!\right] \nabla \times \boldsymbol{E}^{inc}, \tag{4}$$

where $[\![\bullet]\!]$ denotes the jump in the argument across the interface.

Energy conservation require the resultant scattered field $\boldsymbol{E}$ to decline according to Silver-Müller radiation condition

$$\lim_{r\to\infty} r\left[\boldsymbol{\nabla} \times \boldsymbol{E} + jk_0\, \boldsymbol{e}_r \times \boldsymbol{E}\right] = \boldsymbol{0}, \tag{5}$$

as $r \to \infty$, where r is the distance between the center of the object and the actual observation point. Infinite Elements (IE) are used here (in the domain Ω_0^+) to implement Eq. (5).

The variational formulation of the above strong formulation is obtained by multiplying Eq. (1) by a vector test function $\boldsymbol{F} \in \mathbf{W}^*$, integrating over the domain Ω, integrating by parts and using Eq. (4). The corresponding weak formulation can be stated as follows. Find $\boldsymbol{E} \in \mathbf{W}$ such that $B(\boldsymbol{E}, \boldsymbol{F}) = L(\boldsymbol{F})$, where the sesquilinear and antilinear functionals B and L are defined as

$$B(\boldsymbol{E}, \boldsymbol{F}) = \sum_{V=\{\Omega,\Omega_0,\Omega_0^+\}} \left\{ \int_V \frac{1}{\mu_r}(\boldsymbol{\nabla} \times \boldsymbol{E}) \cdot (\boldsymbol{\nabla} \times \bar{\boldsymbol{F}})\, dV - k_0^2 \int_V \hat{\epsilon}_r \boldsymbol{E} \cdot \bar{\boldsymbol{F}}\, dV \right\}, \tag{6}$$

$$L(\boldsymbol{F}) = -jk_0 Z_0 \sum_{V=\{\Omega,\Omega_0,\Omega_0^+\}} \int_V \boldsymbol{J}^{imp} \cdot \bar{\boldsymbol{F}}\, dV - \int_\Gamma \boldsymbol{n} \times (\boldsymbol{\nabla} \times \boldsymbol{E}^{inc}) \left[\!\left[\frac{1}{\mu_r}\right]\!\right] \cdot \bar{\boldsymbol{F}}\, dS, \tag{7}$$

$\forall \boldsymbol{F} \in \mathbf{W}^*$ satisfying the homogeneous equivalents of Eqs. (3) and (4). The bar above the test function, $\bar{\boldsymbol{F}}$, denotes the complex conjugate. Here $\mathbf{W}$ is the space of trial functions defined as

$$\mathbf{W} := \{\boldsymbol{F} \in \boldsymbol{L}^2_{r^{-1}} : \nabla \times \boldsymbol{F} \in \boldsymbol{L}^2_{r^{-1}}, \boldsymbol{e}_r \times (\nabla \times \boldsymbol{F}) - jk_0\boldsymbol{E} \in \boldsymbol{L}^2\}, \tag{8}$$

and $\mathbf{W}^*$ is the space of test functions defined as

$$\mathbf{W}^* := \{\boldsymbol{F} \in \boldsymbol{L}^2_r : \nabla \times \boldsymbol{F} \in \boldsymbol{L}^2_r, \boldsymbol{e}_r \times (\nabla \times \boldsymbol{F}) - jk_0\boldsymbol{E} \in \boldsymbol{L}^2\}, \tag{9}$$

where

$$\boldsymbol{L}^2_{r^{\pm 1}} := \{\boldsymbol{F} : F_r \in L^2(\Omega \cup \Omega_0 \cup \Omega_0^+), r^{\pm 1}\boldsymbol{F}_t \in L^2(\Omega \cup \Omega_0 \cup \Omega_0^+)\}, \tag{10}$$

with F_r and $\boldsymbol{F}_t$ being the radial and transversal (tangential to a sphere centered at the origin) components of the field $\boldsymbol{F}$. Note that a necessary condition for a FE-discretization of the electric field $\boldsymbol{E}$ in order to stay in the space $\mathbf{W}$ is that only the tangential component of $\boldsymbol{E}$ must be continuous across inter-element boundaries, i.e. $\mathbf{W} \in \boldsymbol{H}_{\mathrm{curl}}(\Omega)$. The radar cross section σ is defined as

$$\sigma := \lim_{r\to\infty} 4\pi r^2 \frac{|\boldsymbol{E}_\infty(\boldsymbol{x}) \cdot \boldsymbol{p}_{obs}|^2}{\|\boldsymbol{E}^{inc}(\boldsymbol{x})\|^2}, \tag{11}$$

where $\boldsymbol{E}_\infty(\boldsymbol{x})$ is the scattered electric far-field ,and $\boldsymbol{p}_{obs}$ is the observer polarization. The scattered electric far-field may be obtained from the near-field by the following transformation

$$\boldsymbol{E}_\infty(\boldsymbol{x}) = \frac{k_0}{4\pi\|\boldsymbol{x}\|}\int_{\Gamma_r} [\hat{\boldsymbol{x}} \times \boldsymbol{M} + Z_0 \hat{\boldsymbol{x}} \times (\hat{\boldsymbol{x}} \times \boldsymbol{J}) e^{-jk_0 \boldsymbol{r}\cdot\hat{\boldsymbol{x}}}] dS(\boldsymbol{r}), \tag{12}$$

where Γ_r is a surface enclosing the scatter, $\hat{\boldsymbol{x}} := \boldsymbol{x}/|\boldsymbol{x}|$, $\boldsymbol{r}$ is the current point on the integration surface Γ_r. The vector fields $\boldsymbol{M}$ and $\boldsymbol{J}$ denote surface magnetic and electric currents defined as

$$\boldsymbol{M} := \boldsymbol{E} \times \boldsymbol{n}, \quad \boldsymbol{J} := \boldsymbol{n} \times \boldsymbol{H}, \tag{13}$$

where $\boldsymbol{H} := \frac{1}{j\omega\mu}\nabla \times \boldsymbol{E}$ is the magnetic field.

3 Numerical examples

In this section two numerical examples will be studied. The first consists of an open pipe where the electromagnetic back-scatter is computed using FEM (EM3D), MoM (M-RANDOLPH, which is a apart of the suite of programs within GEMS, see [3]) and PO (FOPOL). The second example is a convergence study of the computed scatter from an infinitesimal thin PEC disc.

3.1 Open pipe

Here the electromagnetic scattering on an open pipe will be calculated. The dimensions of the pipe is $36.0 \times 4.0 \times 0.065$ inches (Length $\times$ Diameter $\times$ Thickness). The pipe is considered as a perfect electrical conductor. The mono-static RCS will be estimated in an azimuth sweep from 0 to 180 degrees, where the x-axis is parallel with the axis of the pipe. The results can be seen in Figs. 1 to 3 for three different frequencies. At an angle perpendicular to the manifold of the pipe all three methods agree; however, when the direction of the impinging wave approaches the direction of the x-axis the error using PO is significant. At lower frequencies MoM agree well with FEM, but at higher frequencies, where more energy is able to enter the pipe, there are some discrepancies between the methods.

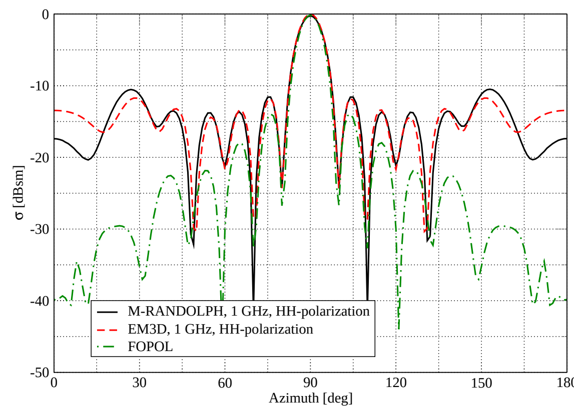

Figure 1: RCS at 1 GHz (HH-polarization).

3.2 PEC disc

In this section the convergence properties of separate and combined polynomial enrichment and mesh refinement methods are studied.

Pure h-refinement and pure p-enrichment convergence rates are compared with hp-refinement. The object under investigation is a PEC disc with infinitesimal thickness and radius $a = 1$. For small wavenumbers an asymptotic series solution is available. The wave number considered here is $ka = 0.5$.

In the case with pure h and p refinement/enrichment algebraic convergences are obtained. As can be seen in Fig. 4, the increase in slope of the convergence rate from using pure p-enrichment instead of pure h-refinement is approximately 1.7. In the case of hp-refinement we obtain almost exponential convergence and far better accuracy than with pure h-refinement and p-enrichment.

Note that the property of interest here is the l_2-norm of the RCS. The reference solution, denoted by σ_{ex}, is obtained using a low frequency analytic series expansion, see [4], and σ_{fe} is the calculated FEM solution. Also note that the initial mesh has to be designed so that the wave is resolved, i.e. it has to fulfill the sampling theorem. The a priori *hp*-mesh was constructed using three h and one p refinement in each sequence, i.e. the last *hp*-refinement, in Fig. 4, consists of three sequences with three h and one p in each sequence.

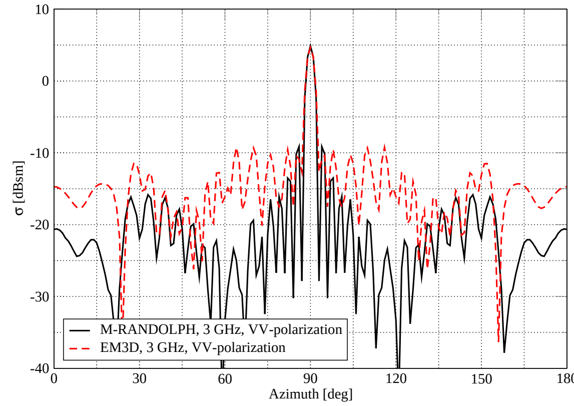

Figure 2: RCS at 3 GHz (VV-polarization).

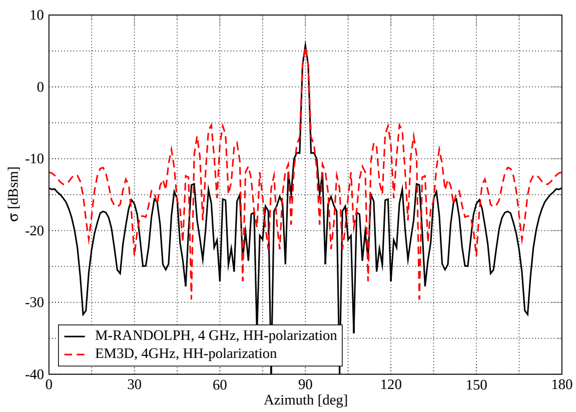

Figure 3: RCS at 4 GHz (HH-polarization).

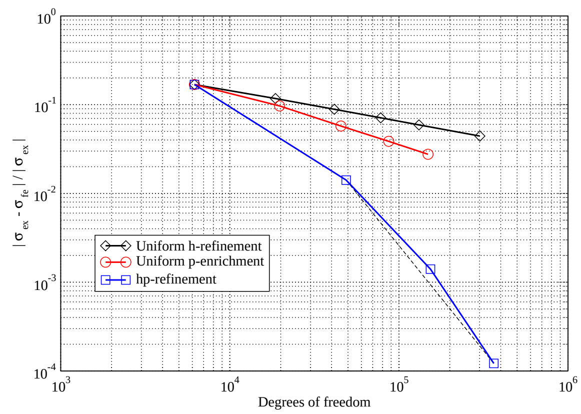

Figure 4: Scattering from a PEC disc, $ka = 0.5$. Far-field convergence of the l_2-norm of the RCS.

4 Conclusion

In this paper the electromagnetic scattering was mainly determined using an *hp*-adaptive version of the FE-Method. When considering a problem with existing singularities it is shown herein, using an infinitesimal thick disc, that the *hp*-approach is superior to traditional approaches such as pure h-refinement and p-enrichment. The convergence rate of the calculated RCS is almost exponential for the *hp*-approach.

References

[1] L. Demkowicz, A. Bajer, W. Rachowicz and K. Gerdes (1999) *3D hp-Adaptive Finite Element Package. Fortran 90 Implementation (3Dhp90)*, TICAM Report 99-29, Texas Institute of Computational and Applied Mathematics, The University of Texas at Austin.

[2] A. Zdunek, W. Rachowicz and N. Sehlstedt (2004) *Compters and Mathematics with Applications*, in press. Toward hp-Adaptive Solution of 3D Electromagnetic Scattering from Cavities.

[3] General ElectroMagnetic Solvers (GEMS). Swedish national project.
`http://www.psci.kth.se/Programs/GEMS/index.html`

[4] J. Meixner and W. Andrejewski, (1950) *Strenge Theorie der Beugung ebener elektromagnetischer Wellen an der vollkommen leitenden Kreisscheibe und an der kreisformingen Offnung im vollkommen leitenden ebenen Schirm*, Annalen der Physik 7, pp 157-168.